

INTRODUCTION TO THE ARCOPTER ARC WING
AND THE BERTELSEN EFFECT FOR POSITIVE PITCH STABILITY AND CONTROL

William D. Bertelsen
Bertelsen, Inc.

SUMMARY

Studies in the realm of low-speed and motorless flight have traditionally produced the most creative approaches to the problem of flight. The problem is the same today as always, namely, the search for higher performance with complete safety. Towards that end a brief report is offered on a new wing design, new in geometry, construction, and flight characteristics. This report includes preliminary wind tunnel data on a three-dimensional model as well as some full-scale man-carrying test results. There are photos of all phases of the experiments and some figures which serve to illustrate the Bertelsen Effect, a unique focus of aerodynamic forces in the arc wing system which allows the attainment of high lift coefficients with the maintenance of pitch stability and control.

INTRODUCTION

The name "Arcopter" comes from a combination of the Latin word "arc" for segment of a circle with the Greek "pteron" for wing. The name thus embodies the basic geometric configuration of the device. In this case the arc refers not to any chordwise airfoil curvature but to a regular spanwise curvature describing an arc like a rainbow over the lateral pitching axis of the system. From antiquity the arch has been an element of structural design and it has come to be a symbol of strength and simplicity. This paper introduces the arc wing configuration as a novel aeronautical device which embodies certain valuable aerodynamic properties in a light-weight, self-constituted physical unit of inherent strength and simplicity.

ABBREVIATIONS AND SYMBOLS

Values are given in both SI and U.S. Customary Units. The measurements and calculations were made in U.S. Customary Units.



VTOL	vertical takeoff and landing
m.p.h.	miles per hour
R.P.M.	revolutions per minute
C.L.	center of lift
C.G.	center of gravity
a.c.	aerodynamic center
L	lift, kg (lbs.)
D	drag, kg (lbs.)
T	thrust, kg (lbs.)
W	weight, kg (lbs.)
α	angle of attack, degrees
x'	lift moment arm, m (ft.)
z	drag moment arm, m (ft.)
c	wing chord length, m (ft.)
V	velocity, m/sec (ft/sec)
C_L	coefficient of lift
C_D	coefficient of drag
C_{Mac}	moment coefficient about a.c.
C_{Mcg}	moment coefficient about C.G.

INVENTION OF THE ARC WING

The VTOL Design Problem

In the 1950's the National Advisory Committee for Aeronautics (NACA) recognized the usefulness of the helicopter because of its ability to operate from very small bases. The advantages to be gained with an airplane that incorporated both the small-field capabilities of the helicopter and the high-speed potential of conventional airplanes became readily apparent (ref. 1). One possible means of achieving these advantages was seen to be an engine/

propeller combination capable of providing static thrust in excess of gross weight. Lift for vertical takeoff could then be obtained by deflecting the propeller slipstream downward by means of large-chord wing flaps, retractable for high-speed cruising flight. Accordingly, an investigation of various wing/flap configurations was conducted in the 7- by 10-foot tunnels at the Langley Aeronautical Laboratory in an effort to develop relatively simple arrangements that could deflect propeller slipstreams downward for vertical takeoff. References 1, 2, and 3 present the characteristics of slotted, sliding, and plain flaps, respectively.

The slotted-flap configuration was effective in achieving a slipstream turning angle corresponding to a rotation of the effective thrust vector upward about 73° , with the ratio of resultant force to thrust varying from about 1.00 nearest the ground to about 0.86 out of the ground effect region. With this configuration it was concluded that vertical takeoff could be made with an initial attitude of 17° and at airplane weights up to 90 percent of the total propeller thrust.

Similar results were achieved with the plain flap configuration, but only after the installation of auxiliary vanes which greatly complicated the arrangement. The slotted-flap configuration, while seen as somewhat simpler, had the disadvantage of exhibiting rather large diving moments, caused partly by the fact that as the flaps extended they moved appreciably rearward and the effective axis of the redirected slipstream was relatively far behind the quarter-chord point of the wing. For the same turning angle the diving moments associated with the slotted-flap configurations were found to be approximately twice as large as the diving moments for the configurations with plain flaps and two auxiliary vanes. However, the process of retracting and storing the two auxiliary vanes necessary on the plain flap system was seen to present serious mechanical problems, nearly prohibitive to the design of a practical, high-speed VTOL aircraft.

Subsequent investigation of the Ryan VZ-3RY VTOL prototype (ref. 4) under the auspices of the new National Aeronautics and Space Administration in 1959 underscored the serious limitations of the conventional approach to the design of double-slotted flaps for VTOL applications. While the aircraft could take off vertically, longitudinal stability was said to be impossible to realize below 46 km/hr (29 m.p.h.) with the existing center of gravity location. Pitch control in hover and transition was difficult and critical even with a complicated jet-reaction control located in the tail.

In summary, the experiments established (1) that VTOL capabilities are possible with slipstream deflection by means of conventional, large-chord, double-slotted flap arrangements and (2) that, because of the large diving moments associated with extended

double-slotted flaps, a VTOL using such an arrangement may be longitudinally trimmed and controlled in either the hovering mode or the transitional mode but not in both, at least not by simple means. A VTOL aircraft should be stable and controllable in hover, transition, and high-speed cruise. Conventional tail surfaces are totally ineffective at zero forward speed and almost ineffective in transition. The NACA-NASA studies of the 1950's indicated that an unconventional approach would be required to meet the VTOL design challenge.

The Arcopter VTOL

The Arcopter wing system was the direct result of the efforts of Dr. William R. Bertelsen to develop a slotted flap configuration for deflecting a propeller slipstream through the large turning angles required for vertical takeoff without the deleterious diving moments or complexity which accompanied the NACA experiments. The cited NACA technical notes touch on the importance of the center of gravity location in analysis of VTOL wing and flap pitching characteristics.

In the Arcopter system it is proposed that if an aircraft extends single or multi-element flaps and/or slats for high lift or slipstream deflection, then those flaps should rotate, while extending, about an area in which the center of gravity lies, so that the summation of flap resultant forces converges at all times in the vicinity of the center of gravity. Each flap may be considered in such regard as an entity with its own force focus coinciding with the others near the center of gravity. The center of gravity is preferably below the center of lift of the airfoil combination in order to effect stability regardless of the attitude of the aircraft with respect to gravity. The concentration of wing forces, coupled with flap and wing slot augmentation, all converging about the center of gravity of the aircraft, thus comprises an engineering principle called the Bertelsen Effect.

Figure 1 shows how multi-element flaps might be arranged to take advantage of this principle in a VTOL of the deflected slipstream type. It can be seen that if flaps B and C retract and extend by pivoting on a radius centered at the C.L./C.G. focal point there will be little or no diving moment at any flap setting. The aircraft can therefore make the transition from hover to flaps-up cruise smoothly and predictably. Because of the focus of flap resultant force through the C.G. area, the system does not depend on propeller thrust to achieve longitudinal trim in any mode. Forces remain balanced at all power settings including power off, affording an extra measure of safety in controlling a power-off descent. The full lifting capability of the wing system can be utilized in all modes without the usual loss in effec-

tive lift coefficient owing to negative tail loads. The need for such negative loads is effectively eliminated in the Arcoputer system.

Figure 1 diagrams the general arrangement of wing and flap elements around the center of gravity. It is left to specify the most practical physical form to be taken by an aircraft which is to employ the Bertelsen Effect. It has been established that multi-element slotted flaps of large chord can deflect a propeller slipstream through the large turning angles required for vertical takeoff (ref. 1). Reference 5 suggests the effectiveness of large end plates in augmenting flap efficiency as regards the ratio of resultant force to thrust, especially in ground effect. The Arcoputer system proposes a synthesis of the wing and end plates into a spanwise, semicircular arc as being the most efficient configuration for confining and deflecting the slipstream of one large-diameter propeller or two dual-rotating propellers on a single thrust axis. At the same time the necessary rotational motion of arc-shape flap elements can be easily achieved, owing to the convenient coincidence of element pivot points on an axis across the diameter of the arc. This location and coincidence of wing element pivots substantially simplifies the mechanism for flap actuation.

Figures 2-6 are photos of the Arcoputer VTOL flying model which was built to demonstrate the Arcoputer design principle and the Bertelsen Effect. Figure 2 shows the arc wing and flap elements fully extended. Such arched structure is inherently strong while being light in weight. Because of the great tensional strength of the arch structure, there is no longer a design requirement for thickness in the structure of the main wing. Airfoils can be chosen without regard for structural considerations. The wing and flaps on the model are constructed of molded Plexiglas sheet. Aluminum tubes attached to the model are for handling and serve no aerodynamic function. Figure 3 shows the complete VTOL model in a three-quarter front view, flaps fully extended. Simple canard control vanes have been included in the slipstream to counteract propeller torque and provide positive three-axis control at all speeds including zero and reverse. It can be seen that any residual diving moment can be dealt with by increasing incidence on the horizontal canards in such a way as to contribute to the overall slipstream-turning and lift effectiveness of the system.

Figure 4 is a direct front view showing shortness of the wingspan. If a single thrust axis is to be used on an Arcoputer VTOL, the wingspan should be somewhat less than the diameter of the prop or rotor. Short span saves weight and reduces drag in high-speed cruise. The tubular diametric spar visible in figure 4 is oversized for rough handling. Figure 5 shows a side view of the Arcoputer VTOL in high-speed cruise configuration with flaps retracted. Thin flap segments easily nest in the main arc wing

after simple rotational motion, pivoting about the diametric axis through the wing tips at the point where the tightening nut attaches the handle. A glow plug engine drives the propeller via an extended shaft to help maintain proper C.G. location. Viewed from the top (fig. 6) the arc wing is seen to have an elliptical planform, and therefore a near-ideal lift distribution.

The Arcopter VTOL model was demonstrated (in and out of ground effect) in hover, in slow flight fore and aft, for control effectiveness, etc., in the 7- by 10-Foot Tunnel at Langley Aeronautical Laboratory on January 23, 1958. As a solution to the VTOL design problem, the Arcopter offers a simpler, safer alternative to the helicopter through implementation of the Bertelsen Effect. But the invention of the arc wing as an element in itself, an arch-tension structure with centralized force focus, offers possible solutions to a variety of aeronautical design problems, especially those where lightness of weight and structural simplicity are prime considerations.

THE ULTRA-LIGHT ARCOPTER WING

As indicated previously, the arc wing may be considered in multi-element combinations, as in the VTOL discussion, or each element may be considered separately as an entity with its own centralized force focus. Figure 7 represents the Bertelsen Effect as it applies to a single-element arc wing. It shows how lift force acts in a direction perpendicular to imaginary lines tangent to each point along the semicircular arc wing span. The magnitude of a local lift force through the point of tangency is proportional to the local wing chord length and angle of attack. On an arc wing with an elliptical planform, the greatest lift will develop near the crown of the arch where the wing chord length is greatest. The vector L represents the relative magnitude and direction of lift force acting on this point with respect to the lift forces which act simultaneously on every other point along the span. Because the arc wing is a semicircle as viewed from the front, it becomes clear that all lift forces, regardless of magnitude, aim through a common point at the geometric center of the arc. This point is the true center of lift in the Arcopter system.

On the right in figure 7 is a side view of the arc wing focus. This side view shows how lift and drag forces interact at each local section center of pressure to focus a resultant force directly through the geometric center of the wing arc. If the aircraft C.G. is also located near this point, the vector sum of the forces is zero, and there is no pitching moment about the C.G. The longer broken lines denote the outline of the arc wing leading and trailing edges as seen from the side. Vector R' has the same magnitude and direction as the resultant R and acts through

the same point. R' is simply a restatement of the resultant R for convenience in graphically adding R to the weight W and thrust T.

Structure of the Ultra-Light Arc Wing

It was decided to design and build a single-element arc wing to analyze its aerodynamic properties, including lift, drag, and static pitch stability. The basic simplicity and tension strength of the arc geometry implied that an ultra-light structure could be devised which could support a very large wing area. Intuitively, the semicircular shape is suited for confining high pressure air underneath the wing surface by effectively restricting spanwise flow. If the wing were properly designed, the lift force created by the free stream should stretch a single- or double-surface fabric membrane into an efficient airfoil curve without the necessity for any rib structure whatsoever, at a great saving of weight, cost, and complexity.

The ultra-light, adjustable-camber arc wing evolved during numerous experiments with models, kites, wind tunnel tests, full-scale force tests, and finally, man-carrying, powered, free-flight tests. The wing is essentially a fabric tension structure utilizing the dynamic force of the air to stretch the wing fabric on the bias, thus maintaining a single-surface airfoil curve. (See figure 8.) An aluminum tube forms the basic arch inside the fabric cuff at the wing's leading edge. This aluminum (or fiber glass) arch is anchored in sockets at opposite ends of a rigid tubular spar. This arch and spar assembly forms a "D" shape unit which has proven extremely rugged and damage resistant on test craft of every size. The sail is patterned after the elliptical planform of the Arcopter VTOL flap elements, with maximum chord length at the crown of the arch.

Maximum chord length was specified arbitrarily to be one-third the length of the wingspan for all size test aircraft, fixing the aspect ratio at about 3.9 to 1. The wing fabric itself is non-porous urethane-coated nylon weighing 88 g/m^2 (2.6 oz/yd^2). There is no continuous rigid structure shaping the wing sail except for the arch tube in the leading edge. At zero airspeed the fabric droops limply from the arch. The only other members required for proper shape in flight are a number of rigid tubes or sticks which extend between the leading and trailing edges of the wing at various stations on the span. The length of each of these chordwise members is adjustable, making it possible to change airfoil camber between flights. Shortening the tube increases the camber. The tubes are all double hinged at their leading-edge point of attachment to allow the sail to hang down at zero forward speed. Nylon webbing straps are sewn to the leading and trailing edge of each wing tip to transfer flight loads to the spar. The trailing edge webbing straps also serve an important pitch control

function to be discussed later.

The preceding description of the ultra-light arc wing structure is brief but complete. It is a supremely simple structure with few parts, but its arc configuration and adjustable-camber surface enable it to develop respectable lift coefficients. At flying speed all waviness and wrinkles disappear as the fabric stretches to its cambered airfoil contour without the use of ribs or battens. The natural load distribution of the arc configuration seems to prevent fluttering of the trailing edge without the need for battens. Also contributing to efficiency is the elimination of the usual fuselage junction losses which disturb most wing mid-sections. The device shown in figure 8 can be built to almost any size without complicating the design. The arc wing photographed in figures 8-10 has a wingspan of 3 m (10 ft.). This unit was used extensively to develop structural design and fabrication techniques, as well as to study pitch stability and control in tethered flight.

Pitch Stability and Control

As apparent in figures 8-10 the Arcopter wing has inherent positive static pitch stability in flight without the addition of auxiliary stabilizing surfaces which most aircraft require. This stability is largely independent of airfoil section characteristics. Any airfoil section can be employed on an arc wing according to performance requirements. Moreover, the angle of attack at which the wing stabilizes can be completely controlled by varying the tension in the trailing edge of the wing. This is easily accomplished by tightening or loosening the nylon webbing strap which anchors the wing fabric to the spar at the trailing edge.

Figure 11 shows the full-size Arcopter wing built to carry a man. Wingspan of this unit is 7.3 m (24 ft.). Clearly visible at the wingtip trailing edge is a steel cable attached to the nylon anchor strap. When the cable is connected to a trim tab crank or control stick, the pilot can control the wing's pitch attitude in flight. Pulling on the cable causes the wing to stabilize at a higher angle of attack. Releasing tension causes the wing to pitch down to a more shallow angle of attack. Recovery from a completely luffed condition resulting from negative angles of attack can be made at once by pulling on the cable. Continuing to draw the trailing edge down results in stabilization at extremely high angles of attack, upwards of 40° . Experience has shown that at high angles of attack the arc wing behaves like a parachute and cannot be stalled in the normal sense. Releasing some tension on the trailing edge produces immediate wing response, restabilizing it at some lower angle of attack. Total cable travel required for the whole flight range is only about 15 cm (6 in.).

Center of Gravity Location

As in the case of the Arcopter VTOL, the pitch stability and control behavior of the ultra-light arc wing is primarily related to the location of the center of gravity with respect to the vector sum of all aerodynamic forces acting on the wing. Figure 12 is a representation of wing and low C.G. location which is somewhat like the arc wing situation. Values can be assigned to the lift moment arm x' and the drag moment arm z for each angle of attack to be considered. The value of x' is taken to be negative when the C.G. lies ahead of the aerodynamic center (a.c.). The value of z is taken to be positive when the C.G. is below the a.c. The formula in figure 12 is developed in reference 6 to express the pitching moment about the C.G. when the C.G. location and relative forces are known. Positive values of $C_{M_{cg}}$ indicate tendency to pitch up and negative values indicate tendency to pitch down.

Using the formula, a family of curves of $C_{M_{cg}}$ versus angle of attack can be developed to predict the basic pitch stability characteristics of a conventional wing with a C.G. located 1.5 chord lengths below the section a.c. Figure 13 is such a plot using coefficient values of an NACA 23012 wing of aspect ratio 6. The angle of attack corresponding to a pitching moment of zero is called the "trim point". The slope of the curve at the trim point is an indication of the static pitch stability of the system; the more negative the slope, the more statically stable the wing. Aft movement of the C.G. results in a trend toward increased stability at higher angles of attack.

Figure 13 is a hypothetical case not meant to represent the exact behavior of an arc wing, but it does indicate the large influence C.G. location has on static pitch stability. Minor adjustments in C.G. location might be made accordingly which would enable an arc wing to use any airfoil section and yet retain a zero pitching moment about the C.G. at the design lift coefficient. When the C.G. is fixed, minor shifts in the focal position of the force vectors (from changes in trailing edge tension) give total pitch control on the ultra-light arc wing.

Preliminary Wind Tunnel Tests

Through the cooperation of the late Dr. H.S. Stillwell, then head of the University of Illinois Department of Aeronautical and Astronautical Engineering, a brief series of tests were conducted on a single-element arc wing of ultra-light construction in the university's 1.5-m by 1.5-m (5 ft. by 5 ft.) low-speed wind tunnel in 1973 and 1975. The 1975 data is included in figures 14 and 15. Figure 16 shows the model installed inverted in the test facility. Wingspan was 1.2 m (4 ft.). The model was of the same construction in all respects as described previously, including the wing

fabric of non-porous urethane nylon, sewn to allow some bias stretch.

Several problems combined to interfere with the accuracy of the test results. In the first place, the model was perhaps too large for the tunnel. Secondly, the smooth airfoil camber which characterizes all the larger arc wings failed to develop on the small wind tunnel model. Thirdly, during the course of the testing, the tunnel screens were discovered to be dirty, thus creating extra turbulence. The screens were removed for the tests labeled "MAX" and "MED" camber in figures 14 and 15. This raised the tunnel Reynolds number based on mean geometric chord from about 0.24×10^6 to 0.32×10^6 . Nevertheless data was taken and tabulated for values of C_L , C_D , and $C_{M_{cg}}$ for three varying degrees of airfoil camber, the extremes of which can be seen in figures 17 and 18. Because of inability of the fabric to stretch naturally into airfoil camber on the small model, it had to be induced by bending the three most central chordwise tubes.

The lift and drag measurements indicated disappointing performance by the model compared with expectations based on experience with the large arc wings in the field. However the maximum value of C_L did show increase with increasing camber as might be expected. One interesting result was that the wing never reached the stalling point in any of the tests. Limitations of tunnel balance apparatus precluded investigation of very high angles of attack, but it can be seen in figure 14 that the wing with maximum camber did not stall even after a 29° increase in attack angle, beginning at C_L of about 0.23.

The pitching moment data (fig. 15) taken about the horizontal spar shows a negative slope, indicating a degree of positive static pitch stability, in all three tests. Increasing airfoil camber appears to produce greater positive (nose-up) values of the C.G. moment coefficient at low angles of attack. Positive moments remain near the maximum even in the vicinity of the zero-lift angle. Unfortunately, angles of attack below the zero-lift angle were not investigated. The pitching moment data implies that the arc wing will retain a measure of positive static stability about the C.G. no matter what airfoil curvature is employed. Increased camber seems to have a favorable effect on static stability.

Piloted Tests of the Full-Scale Arc Wing

By 1976 the 7.3 m (24 ft.) span Arcopter wing was ready for limited flight testing with a pilot aboard. The wing itself, as shown previously in figure 11, of projected area 13.9 m^2 (150 ft^2), was fitted to a heavy-duty tricycle landing gear for auto towing.

In addition, a unique annular rudder-elevator provided yaw control and contributed to pitch control (fig. 19). Like the wing, the "ring tail" is a light-weight tension structure with a circular rigid hoop inside the fabric cuff at the leading edge. In the same manner as the wing, the tail design provides a maximum of effective area with a minimum of structure.

The auto-tow tests of the Arcopter "sailplane" were very limited, intended only to gauge the minimum flying speed at gross weight. On one such experiment observed by Dr. Stillwell, the wing lifted a total of 170 kg (375 lbs.) at 10.7 m/sec (24 m.p.h.). No drag measurements could be made, but the low-speed lifting potential of the full-scale wing was substantiated. Some pilotless tethered flying was also conducted in moderate wind of 8.9 m/sec (20 m.p.h.), as shown in figure 20. Empty weight was 107 kg (235 lbs.). These tethered flights indicated the wing to be so stable in pitch at moderate to high angles of attack that the ring tail could not effect any visible change in pitch attitude. Subsequently all pitch control was accomplished by regulating trailing edge tension according to the method described earlier.

In an attempt to come as close as possible to full-scale flight conditions for the purpose of measuring drag on the Arcopter sailplane, a trailerized mobile force balance was constructed in 1977. The complete airframe, including pilot, was mounted on an articulated steel pylon via a ball-and-socket joint at the aircraft C.G. (figs. 21, 22). The airframe was thus free to pivot about three axes, making it possible to check out control systems as well as to monitor and record airspeed and drag values from calibrated pressure gauges connected to small hydraulic cylinders. Cylinder pressure, being a function of the total drag, was continuously recorded on movie film, as was airspeed from a boom-mounted pitot tube. It was also intended to measure lift with the trailer apparatus but the lift balance failed to function in the predicted manner.

Good drag data was obtained by towing the rig on smooth blacktop. The aircraft was set to stabilize at an angle of attack of 13-15° so a plot could be made of drag versus airspeed. Two days of testing produced the data presented in figure 23. On a number of test runs the arc wing itself was removed from the rest of the airframe in order to measure and compare drag on pilot and supporting structure alone. The resulting figures could then be subtracted from the total drag to gain a more meaningful idea of the drag on the wing as a separate entity. The drag figures obtained on the Arcopter sailplane were low enough to suggest that a very small engine would be sufficient to propel the aircraft and pilot in flight, without necessitating an increase in wingspan.

Besides facilitating drag measurement, the mobile force balance made it possible to safely observe the behavior of the 7.3 m



arc wing at speed. The ball-and-socket coupling at the C.G. allowed the entire aircraft adequate freedom to pitch, roll, and yaw. Test runs were made with and without the ring tail at various speeds in an attempt to ascertain general handling qualities and control responses. The following conclusions were drawn concerning stability: 1. Without the ring tail, the arc wing has only neutral static yaw stability. 2. The arc wing has positive static pitch stability over a wide angle of attack range, with or without the ring tail. 3. The arc wing is neutral in roll stability, but gets increasingly positive as the C.G. is lowered below the center of lift focus. There is no damping in roll. To effect roll control, the arch structure was hinged on wingtip "toggles" to enable the pilot to shift the entire wing and center of lift to the right and left relative to the C.G., but response was sluggish and inconsistent. Pilot weight shift did produce a slow but sure response without adverse yaw.

The Powered Ultra-Light Arcopter B-1A

The experiments conducted with the Arcopter sailplane were important, but certainly not exhaustive. The relative merits of the differing degrees of camber available in the adjustable-camber wing were not explored. But it was proven that the 7.3-m arc wing can carry significant pay loads at low speed. Some evidence was obtained also that power requirements for takeoff are low even with a fairly short wingspan. Piloted flights, powered by a small engine, now more certainly establish the efficiency of the ultra-light arc wing as a lifting device.

The powered Arcopter B-1A was built using the same size wing and tail surface but with a simpler structure supporting the pilot in a prone position on a steel cable anchored at the wingtips. While being lighter and more streamlined, this design has the added advantage of being collapsible for car-top transport. Before installation of the power system and landing gear, the new airframe made piloted tethered flights as a foot-launched hang glider (fig. 24). Empty weight of this configuration, including pilot harness and ring tail, is only 39.9 kg (88 lbs.). Flights out of ground effect were made with a wind of 8.9 m/sec (20 m.p.h.) sustaining a gross weight of 104 kg (230 lbs.), indicating a lift coefficient of 1.5. Angle of attack at the maximum chord station was 13° with respect to the horizon as measured from other photos. The attainment of lift coefficients near 2.0 seems a reasonable possibility, given a modest increase in angle of attack.

The Arcopter B-1A (figs. 25-28) has now made successful short flights, out of ground effect, under its own power with a pilot aboard. Gross weight was 147 kg (325 lbs.). The nucleus of the power system is a small 2-cycle engine of 134 cm^3 (8.2 in^3) dis-

placement which drives two opposite-rotating pusher propellers, each 1.07 m (42 in.) in diameter (fig. 27). A maximum of 45 kg (100 lbs.) static thrust is available at 6500 engine shaft R.P.M. for takeoff and climb. Minimum takeoff airspeed is about 10 m/sec (22.3 m.p.h.).

Future Experiments

Flight testing of the Arcoputer B-1A has only just begun, and experiments will continue. More investigation is warranted because the first flights of the B-1A show that the Arcoputer wing configuration offers a maximum of performance from a minimum of structure, with possible aeronautical utility ranging from ultralight sport flying to high-speed VTOL transportation.

REFERENCES

1. Kuhn, Richard E.; and Draper, John W.: Investigation of Effectiveness of Large-Chord Slotted Flaps in Deflecting Propeller Slipstreams Downward for Vertical Take-Off and Low-Speed Flight. NACA TN 3364, 1955.
2. Kuhn, Richard E.; and Spreeman, Kenneth P.: Preliminary Investigation of the Effectiveness of a Sliding Flap in Deflecting a Propeller Slipstream Downward for Vertical Take-Off. NACA TN 3693, 1956.
3. Kuhn, Richard E.; and Draper, John W.: An Investigation of a Wing-Propeller Configuration Employing Large-Chord Plain Flaps and Large-Diameter Propellers for Low-Speed Flight and Vertical Take-Off. NACA TN 3307, 1954.
4. James, Harry A.; Wingrove, Rodney C.; Holzhauser, Curt A.; and Drinkwater, Fred J. III: Wind-Tunnel and Piloted Flight Simulator Investigation of a Deflected-Slipstream VTOL Airplane, the Ryan VZ-3RY. NASA TN D-89, 1959.
5. Kuhn, Richard E.: Investigation of Effectiveness of a Wing Equipped With a 50-Percent-Chord Sliding Flap, a 30-Percent-Chord Slotted Flap, and a 30-Percent-Chord Slat in Deflecting Propeller Slipstreams Downward for Vertical Take-Off. NACA TN 3919, 1957.
6. Dommasch, Daniel O.; Sherby, Sydney S.; and Connolly, Thomas F.: Airplane Aerodynamics. New York: Pitman Publishing Corporation. Third Edition, 1961.

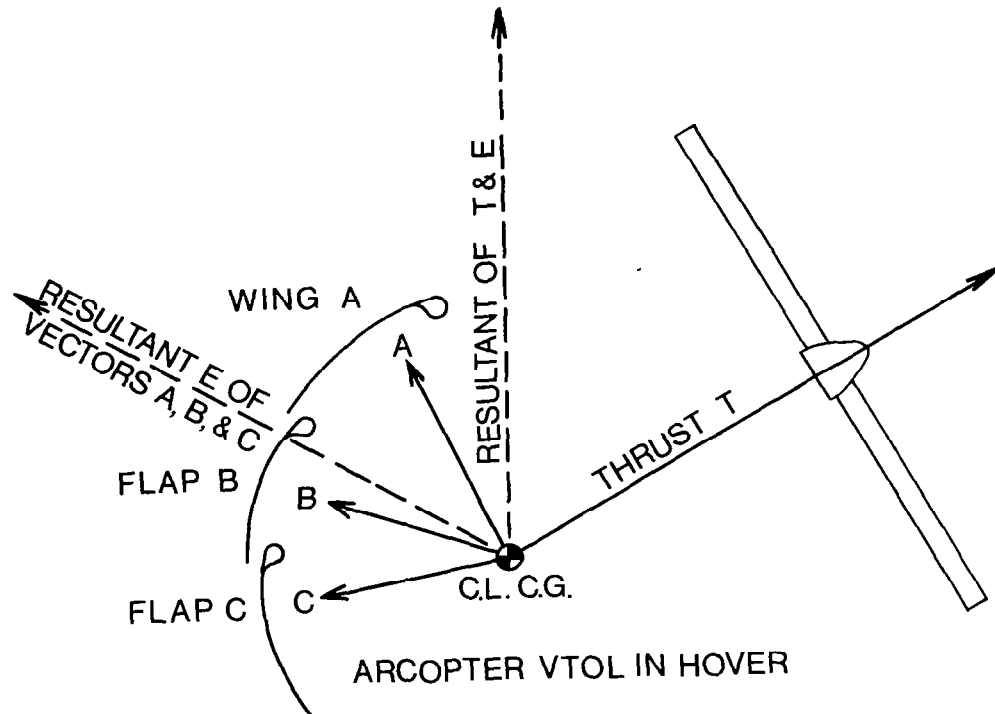


Figure 1.- The Bertelsen Effect, multi-element focus.



Figure 2.- Arcopter VTOL model, flaps fully extended.

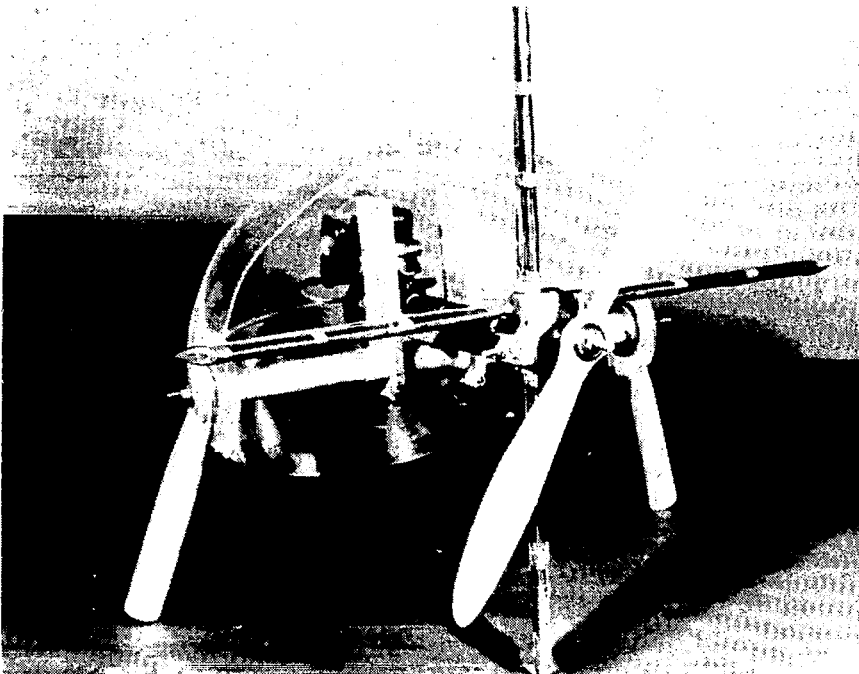


Figure 3.- Arcopter VTOL model,
with canard control vanes.

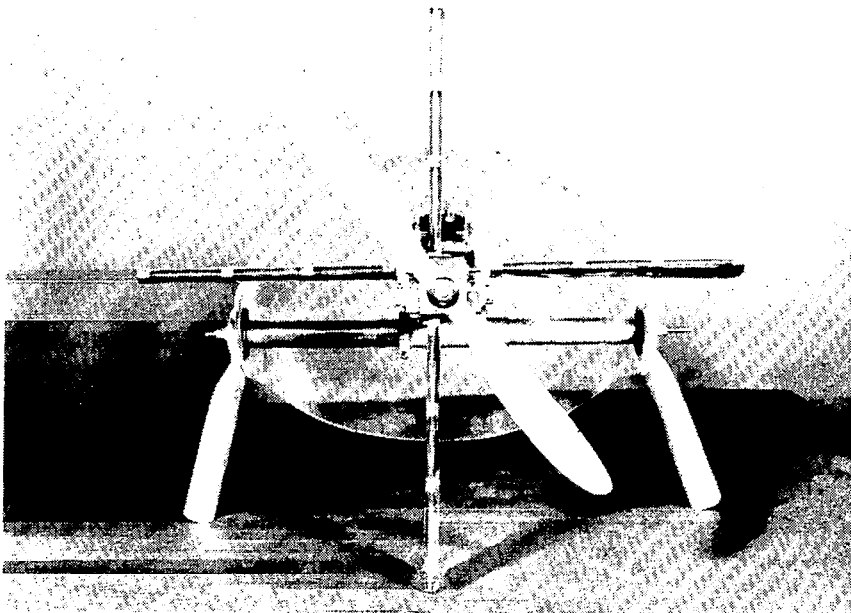


Figure 4.- Arcopter VTOL model (front view).



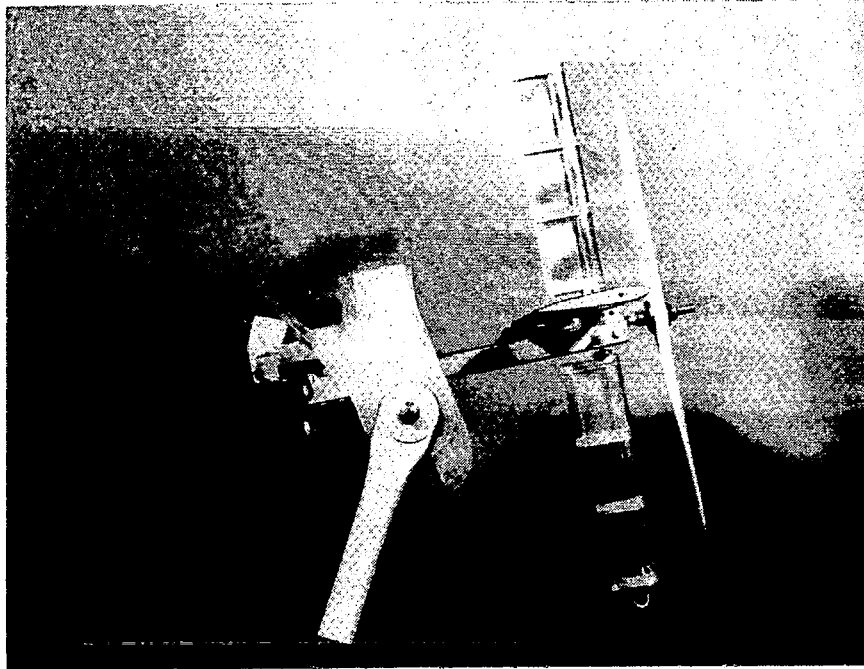


Figure 5.- Arcopter VTOL model, flaps retracted for cruise.

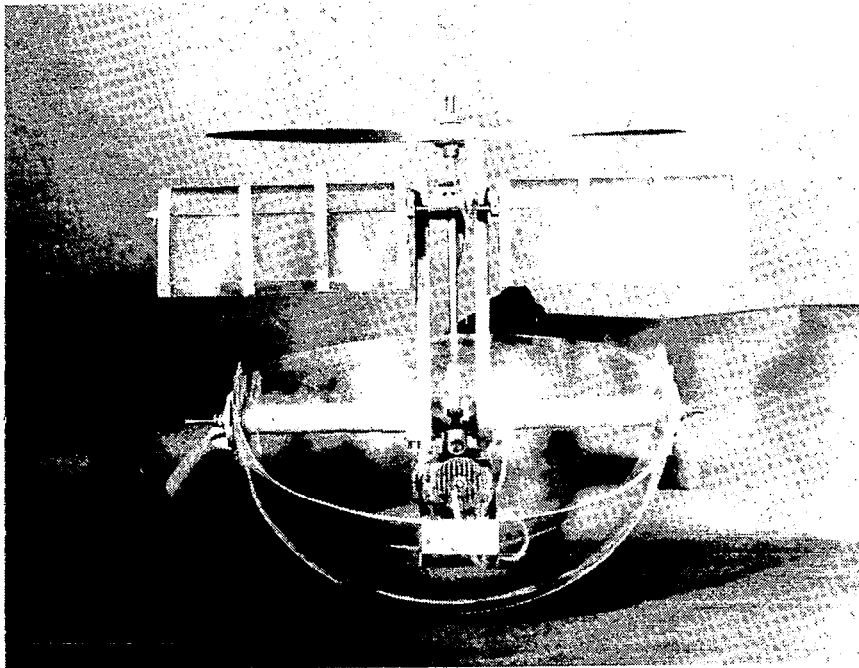


Figure 6.- Arcopter VTOL model, elliptical planform wing (top view).

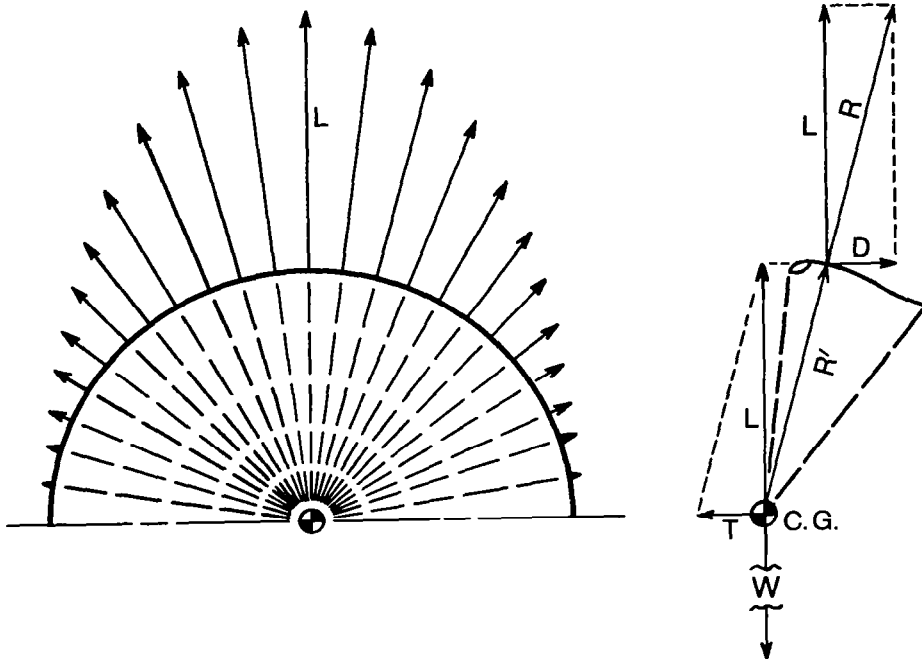


Figure 7.- Arc wing forces, single-element focus.

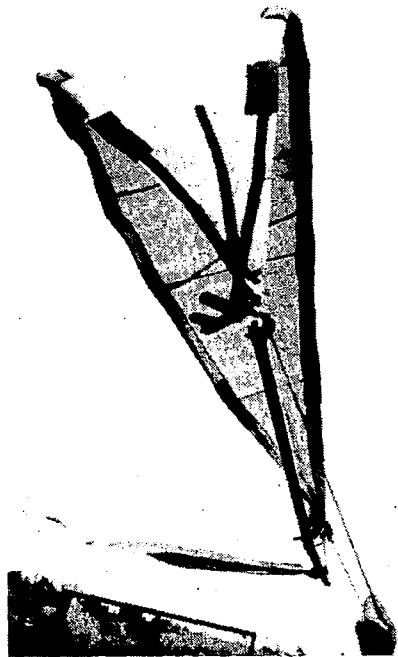


Figure 8.- Ultra-light arc wing,
3-m (10 ft.) wingspan.

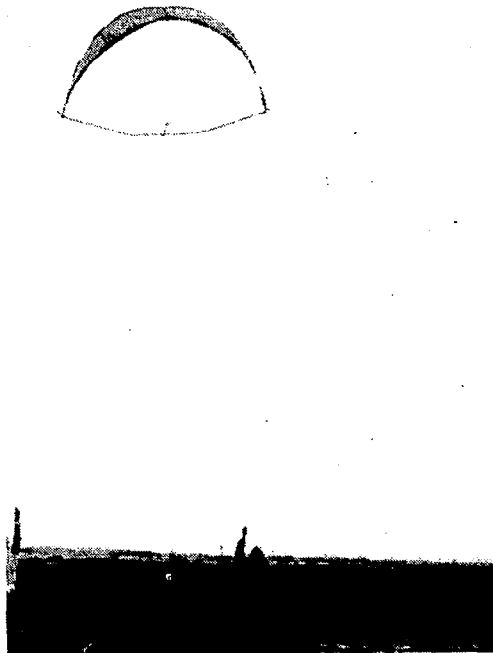


Figure 9.- 3-m arc wing,
pitch-stable flight.

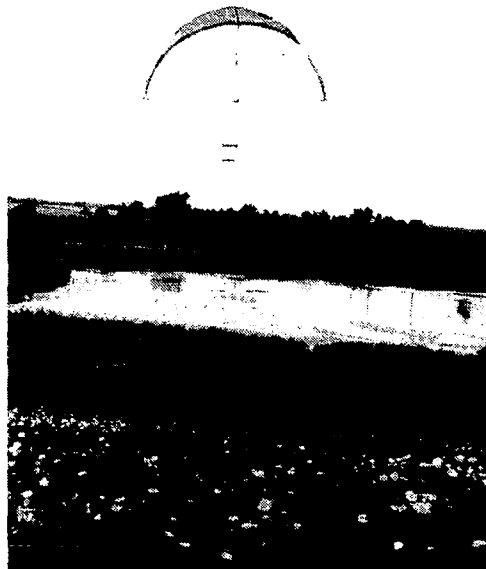


Figure 10.- 3-m arc wing, tethered
flight with payload.



Figure 11.- 7.3-m (24 ft.) arc wing, pitch control detail.

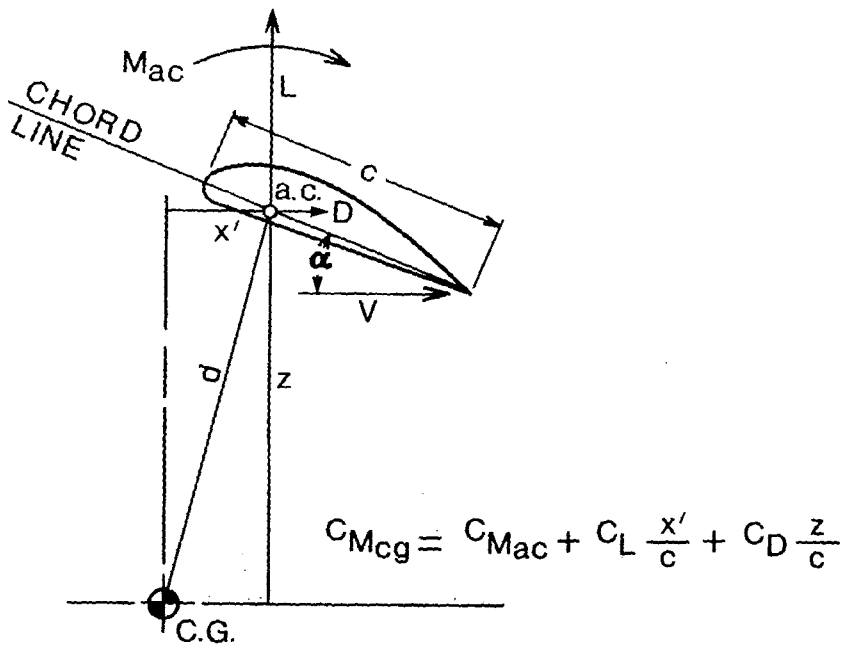


Figure 12.- Moment relation of wing and low C.G.

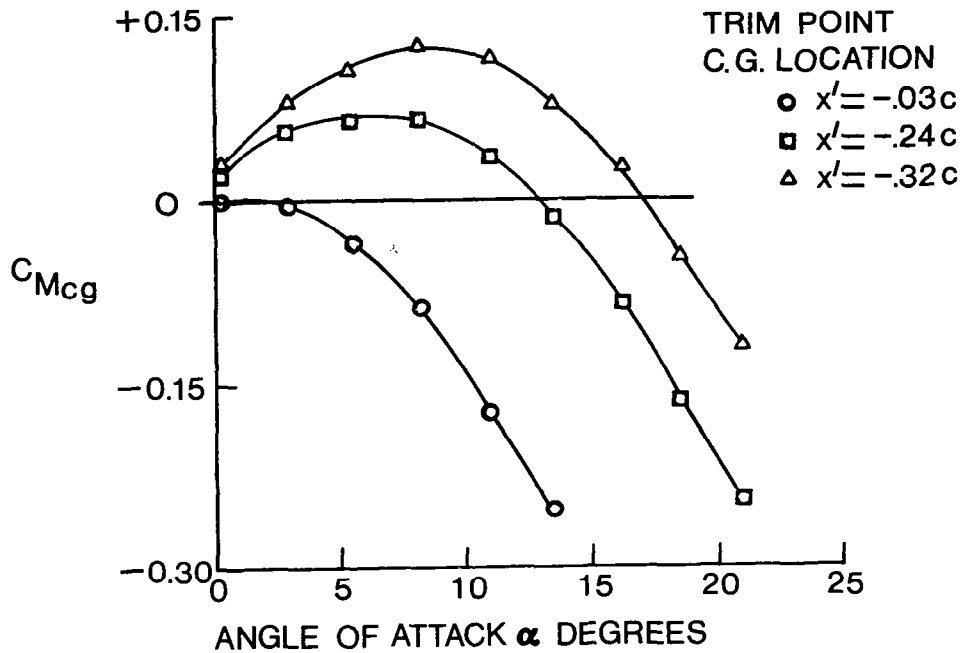


Figure 13.- Pitching moment of wing with low C.G.

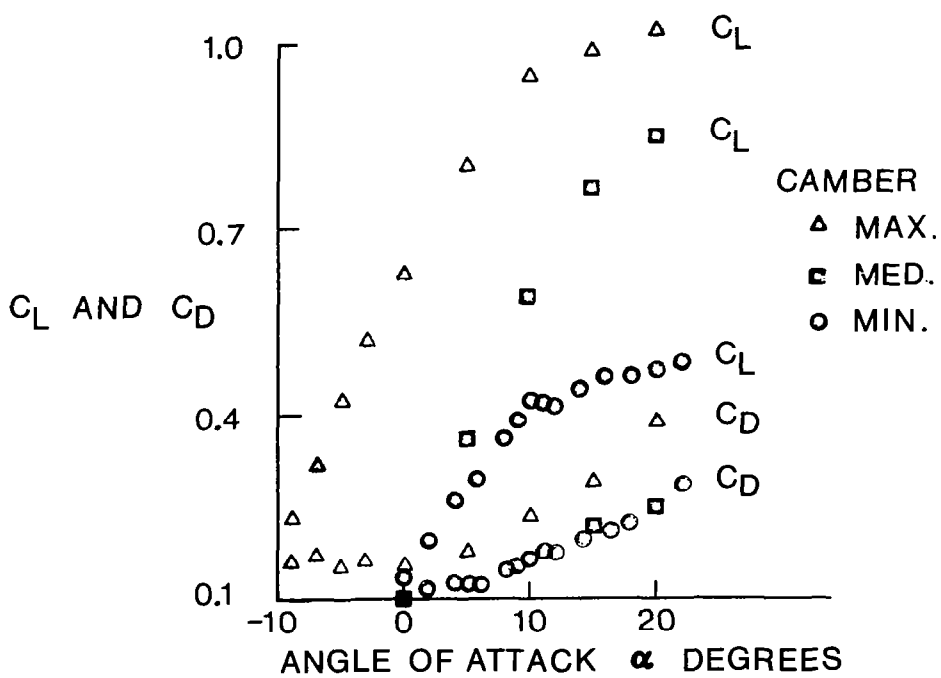


Figure 14.- Arc wing lift and drag (wind tunnel data).

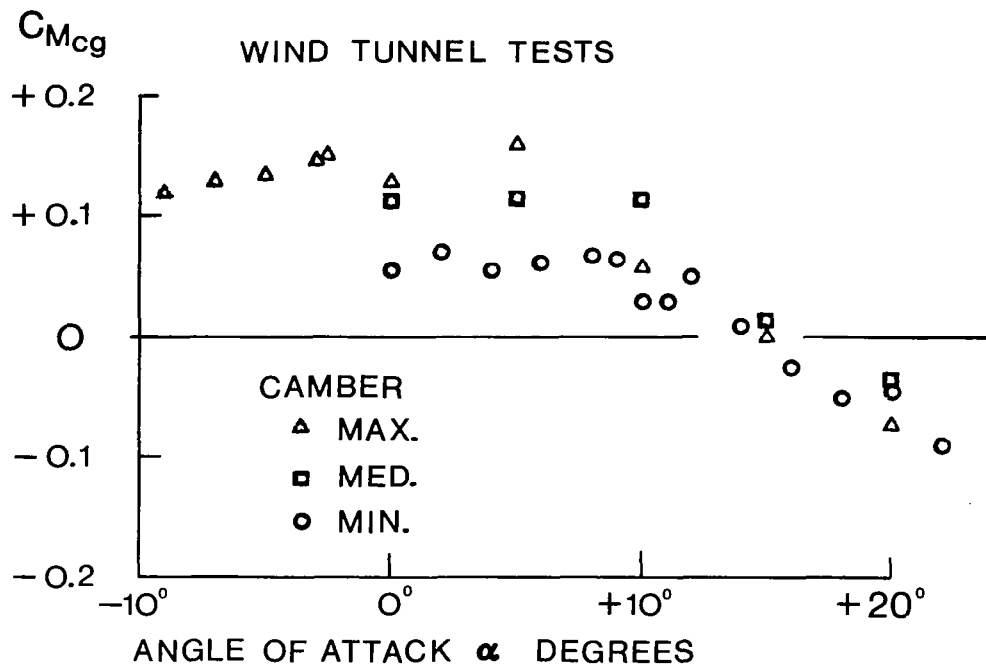


Figure 15.- Arc wing pitching moment (wind tunnel data).

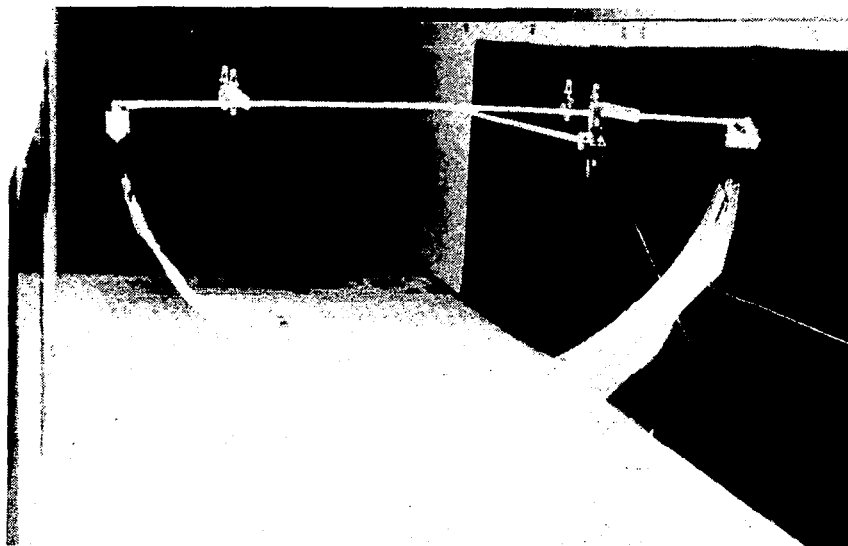


Figure 16.- 1.2-m (4 ft.) arc wing in wind tunnel.



Figure 17.- Wind tunnel test,
minimum camber.

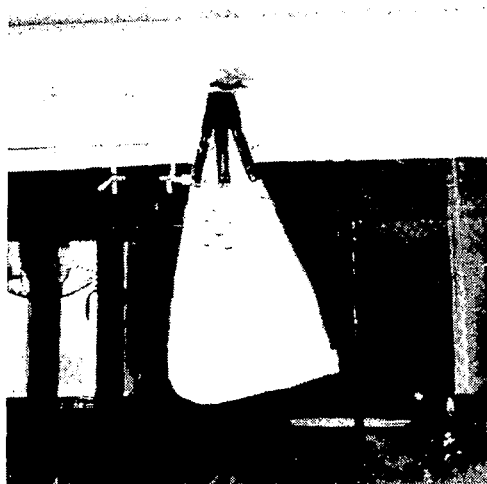


Figure 18.- Wind tunnel test,
maximum camber.

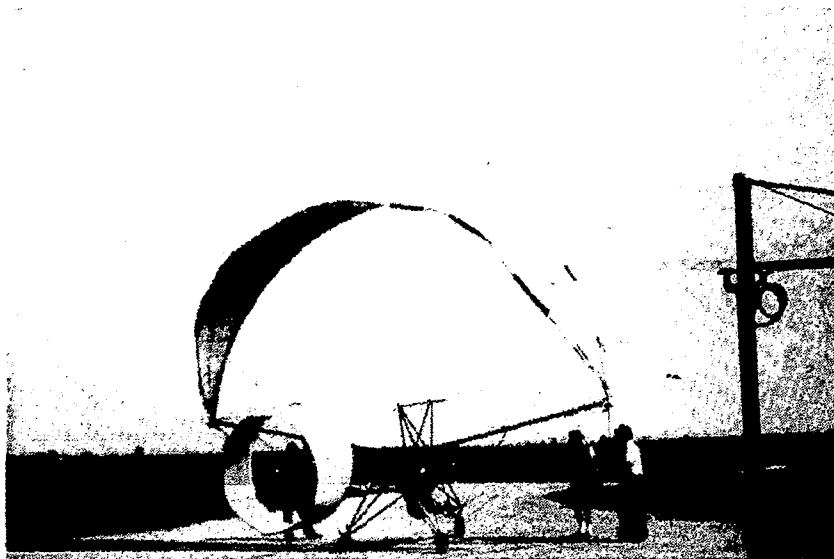


Figure 19.- Arcopter 7.3-m sailplane,
ready for tow.



Figure 20.- Arcopter 7.3-m sailplane,
tethered flight.

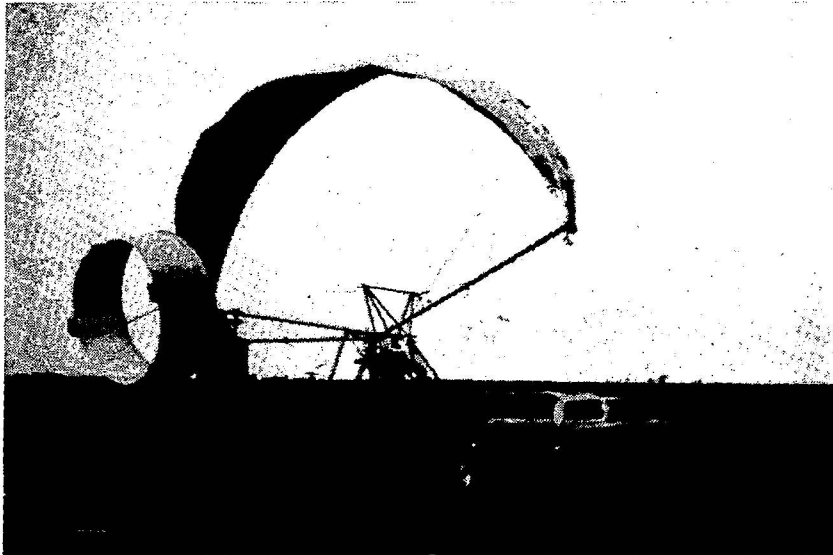


Figure 21.- Arcopter sailplane on mobile force balance.

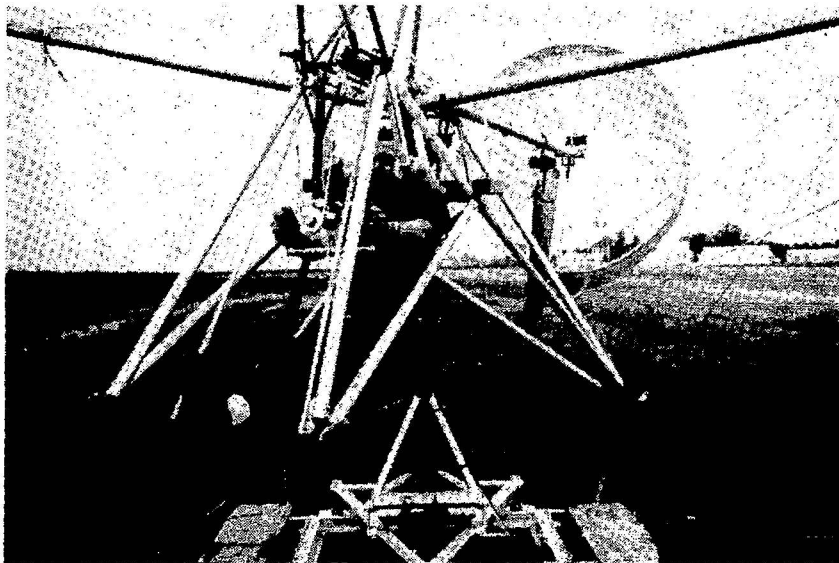


Figure 22.- Arcopter and pilot on mobile force balance, detail.

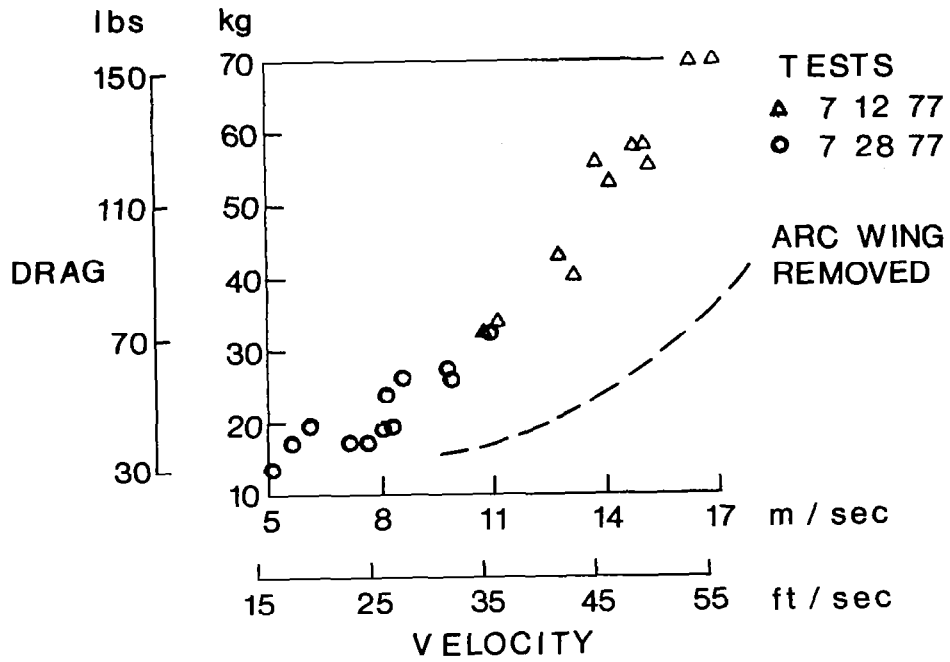


Figure 23.- Total drag of arcopter sailplane (mobile balance data).

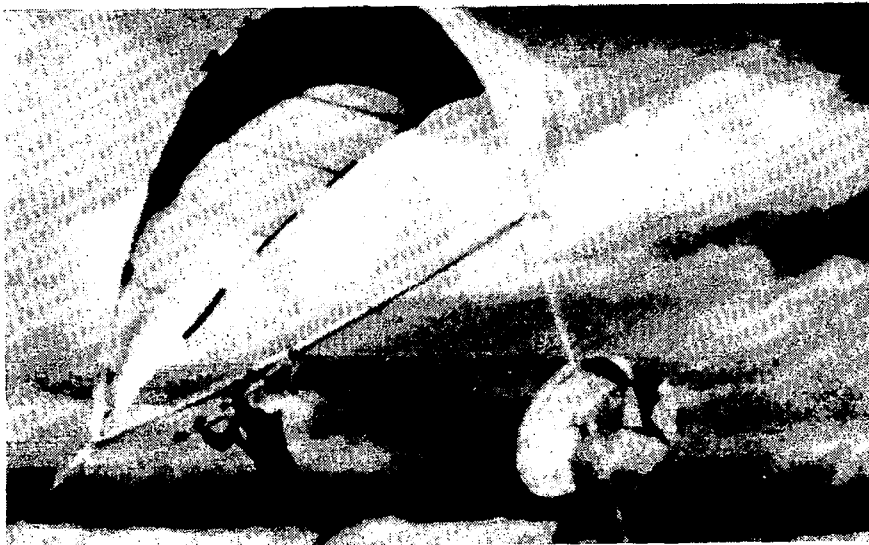


Figure 24.- Arcopter foot-launched sailplane, tethered flight.



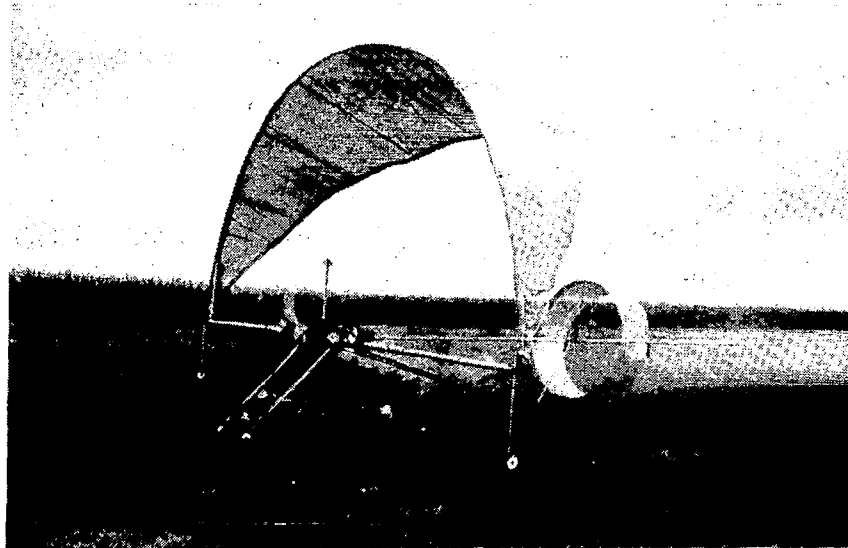


Figure 25.- Arcopter B-1A powered
ultra-light aircraft.

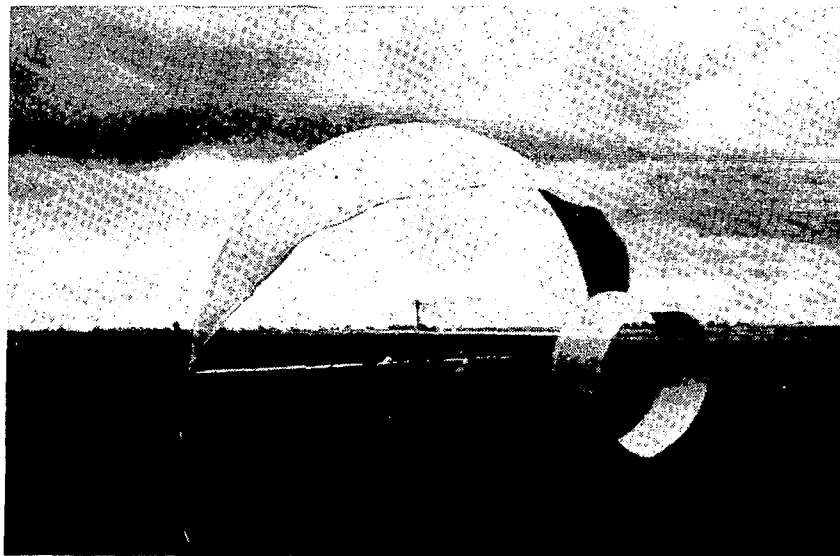


Figure 26.- Arcopter B-1A, empty weight
82.5 kg (181 lbs.).

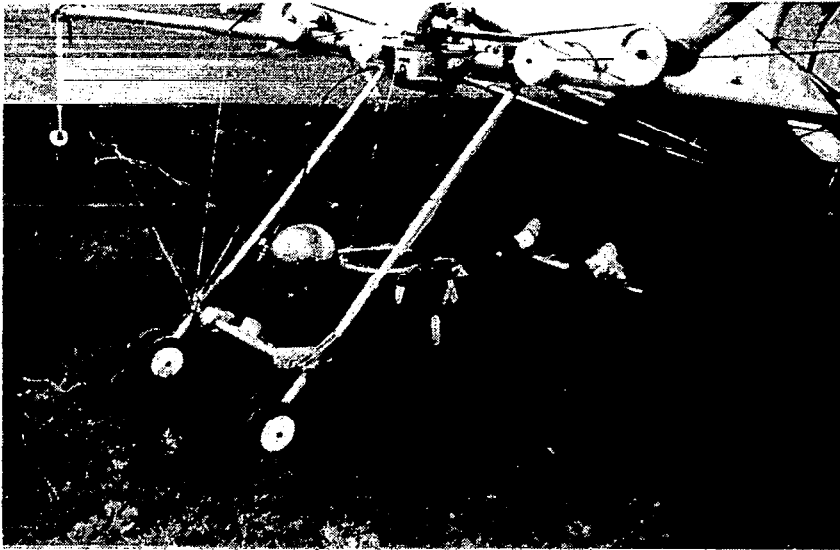


Figure 27.- Arcopter B-1A, power system detail.

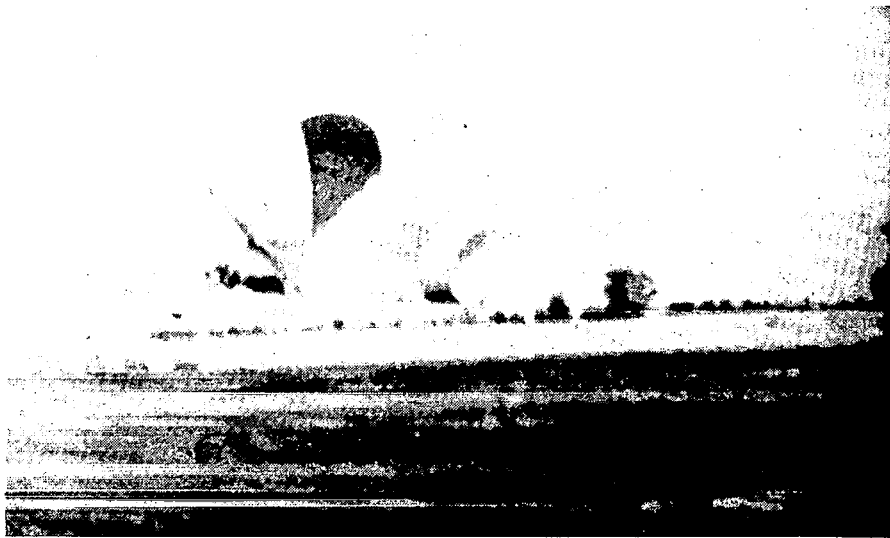


Figure 28.- Arcopter B-1A in powered flight.

